



Article

Distribution of Magnetic Field in 400 kV Double-Circuit Transmission Lines

Ramūnas Deltuva *  and Robertas Lukočius 

Faculty of Electrical and Electronics Engineering, Kaunas University of Technology, LT-51367 Kaunas, Lithuania; robertas.lukocius@ktu.lt

* Correspondence: ramunas.deltuva@gmail.com; Tel.: +370-612-98623

Received: 24 March 2020; Accepted: 1 May 2020; Published: 8 May 2020



Abstract: A high-voltage AC double-circuit 400 kV overhead power transmission line runs from the city of Elk (Poland) to the city of Alytus (Lithuania). This international 400 kV power transmission line is potentially one of the strongest magnetic field-generating sources in the area. This 400 kV voltage double-circuit overhead transmission line and its surroundings were analyzed using the mathematical analytical methods of superposition and reflections. This research paper includes the calculation of the numerical values of the magnetic field and its distribution. The research showed that the values of the magnetic field strength near the international 400 kV power transmission line exceed the threshold values permitted by relevant standards. This overhead power line is connected to the general (50 Hz) power system and generates a highly intense magnetic field. It is suggested that experimental trials should be undertaken in order to determine the maximum values of the magnetic field strength. For the purpose of mitigating these values, it is suggested that the height of the support bars should be increased or that any individual and commercial activities near the object under investigation should be restricted.

Keywords: magnetic field strength; magnetic flux density; magnetic potential; current density; power transmission line

1. Introduction

The institutions involved in electric power transmission in Lithuania and Poland have decided to implement the electricity link “LitPol Link”. This link is designed to connect the power systems of the Baltic States to those in Western Europe and also contributes to the development of the general European electricity market as well as boosting the reliability of the power supply. In pursuit of increasing the capacities of electric power transmission, the decision was made to supplement the LitPol Link by installing an extra 400 kV high-voltage AC double-circuit transmission line.

Recently, there has been increasingly widespread concern over the influence of the electromagnetic field (50 Hz) on the health of residents. One of the fundamental challenges is ensuring safe conditions for those living in locations where such an electromagnetic field is present.

The recently adopted Hygiene Standard HN 104:2011 “Human protection against electromagnetic fields caused by overhead power lines” is currently valid in the European Union (EU) and states that the effective values of the magnetic field strength must never exceed exceed 32 A/m or 40 μ T (magnetic flux density) in residential environments, or 16 A/m or 20 μ T (magnetic flux density) within residential and public service buildings. These values should never be exceeded irrespective of the duration of a person’s exposure to an electromagnetic field.

The double-circuit 400 kV power transmission line is one of the most powerful electrical installations in the entire power system; at a frequency of 50 Hz, it generates an intense magnetic field. Therefore, it is necessary to focus on the installation and safe operation of the 400 kV double-circuit

overhead transmission line in order to prevent the magnetic field generated by this power transmission line from exceeding the requirements set by the European Union (EU) Hygiene Standard HN 104:2011.

2. Extra High-Voltage Double-Circuit Electric Power Transmission Line

As the strongest magnetic field in the electrical power system can be generated by the double-circuit 400 kV power transmission line, it is necessary to determine how the magnetic field is distributed in the surroundings of this overhead power transmission line.

This paper determines a three-bundled, double-circuit 400 kV AC power transmission line. Figure 1 shows a power transmission line of the low-reactance orientation type. The height of conductors shown in the figure is the maximum sag position. The lowest conductors are C_1 and C_2 at the height of 10 m above the ground surface level [1]. Each phase conductor is 0.04 m in diameter. The overhead ground wire has a diameter of 0.015 m.

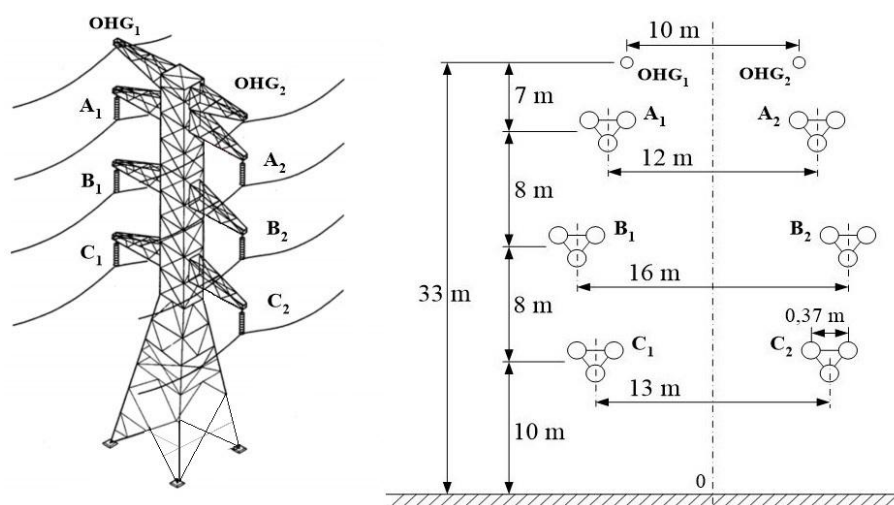


Figure 1. High-voltage double-circuit: three-bundled transmission line.

The height of the 400 kV transmission line supports is 54 m. In this particular case, the lower-phase wires (C_1 and C_2) (see Figure 1), including their insulators, should be arranged at a height of at least 26 m to the ground surface. The sag of the transmission line amounts for 16 m. Adjacent support-bars are spaced by 350 to 550 m [2].

The magnetic field generated by the 400 kV overhead transmission line can be approached as the superposition of the magnetic fields of six long, thin current leads. It is also possible to calculate this magnetic field analytically. As the current leads of the 400 kV overhead transmission line are very long and thin wires, difficult mathematical equations are derived for the purpose of calculating the magnetic field they generate.

Moreover, as regards the effect on humans and the environment, the distribution of these current leads is of utmost importance. However, typical analytical mathematical equations for the calculation of this magnetic field are also missing. Thus, digital modeling should be selected as the main method for the investigation of the magnetic field generated by the 400 kV overhead transmission line [3–6]. Besides the multitudes of advantages it possesses, modeling also enables the simple assessment of the change in the magnetic field when varying the structure and dimensions of the installation. It also allows the different irregularities and variations of the surroundings to be taken into account. Analytical mathematical equations for the calculation of the magnetic field generated by the double-circuit 400 kV overhead transmission line were derived with the aim of verifying the results of modeling [7–16].

3. Magnetic Field Generated by the Single Thin Current Lead

As the double-circuit 400 kV transmission line is comprised of six long, thin current leads, the magnetic field generated by it can be calculated using the method of superposition. We therefore analyze how the magnetic field generated by a single current lead can be calculated. When the magnetic permeability of all points in the space is the same and equal to the permeability of free space μ_0 , the calculation of the magnetic field of the given symmetric current system uses the LaPlace–Poisson equations. When current is passed through the current lead with the element $id\mathbf{l}$, the length is l_i if r represents a radius-vector pointing from the current element $id\mathbf{l}$ to the point of observation, and the electrical current is distributed within the volume of the current lead V_j , the vectors of the magnetic field strength \mathbf{H} and of the magnetic field density \mathbf{B} at the point of observation M are calculated as follows [17–22]:

$$\mathbf{H} = \int_{V_j} d\mathbf{H}; d\mathbf{H} = \frac{(\mathbf{r}\mathbf{J})dV}{4\pi r^3}; d\mathbf{H} = \frac{JdV}{4\pi r^2} \sin \angle \mathbf{r}, \mathbf{J}; \mathbf{B} = \mu_r \mu_0 \mathbf{H}. \quad (1)$$

The magnetic field generated by the current lead can be calculated using a vector potential. When the electric current flows through the lead, making a circuit l_i , and the element $d\mathbf{l}$ and electric current density \mathbf{J} within the volume of the current lead V_j are known, the vector potential \mathbf{A} is expressed as follows:

$$\mathbf{A} = \int_{V_j} \frac{\mu_r \mu_0 \mathbf{J} dV}{4\pi r}. \quad (2)$$

The density of the magnetic field generated by all the current elements $id\mathbf{l}$ of the current lead is expressed based on the superposition principle by summing up the constituents of the flux generated by individual current elements [7–15,23].

Due to axial symmetry, the magnetic field strength line of a long and thin current lead with an electric current passing through it have a circular shape, with their centers on the geometrical axis of the current lead, and they are located in planes that are perpendicular to this axis. At any point of such a circle, the directions of the magnetic field strength vector \mathbf{H} and distance element $d\mathbf{l}$ match.

4. Analysis of Magnetic Field from 400 kV AC Power Transmission Line

In this challenging task regarding magnetic fields, the vectors of magnetic flux density \mathbf{B} or magnetic field strength \mathbf{H} are found to be functions of coordinates when the dependency of the current density vector \mathbf{J} on coordinates is known. As the magnetic field strength or magnetic flux density is to be found in areas in which there are no currents, LaPlace's equation is solved for the scalar magnetic potential. Such a magnetic field will also be of a potential nature [7–15,23].

For the purpose of solving this task, the method of reflections is used. The magnetic field of the conductor system in the double-circuit 400 kV overhead transmission line is examined when the conductor system is comprised of long, thin, round cylindrical conductors running in parallel and with flat conductive surfaces with the symmetrical current systems i_{i1} ($i_1 = A_1, B_1, C_1$) and i_{i2} ($i_2 = A_2, B_2, C_2$) (see Figure 2). The radii of current leads $r_i \ll h_i$ are significantly lower than the distance from the ground surface to the current leads. The sag of the double-circuit overhead power line is not taken into consideration.

Following the method of reflections, the magnetic field in which the distribution of currents over the flat surface of the conductor is known is replaced with the magnetic field of currents i_{in} and that of their reflections- i_{in} . It is assumed that the distances from the conductors i_{in} to their respective reflections- i_{in} are equal; i.e., y_{in} ($i = A, B, C$) ($n = 1, 2$).

With the values of the currents $i_{A1}, i_{B1}, i_{C1}, i_{A2}, i_{B2}, i_{C2}$ being known, the values of reflections of these loads- $i_{A1}^*, -i_{B1}^*, -i_{C1}^*, -i_{A2}^*, -i_{B2}^*, -i_{C2}^*$ are assumed to have the opposite signs.

In order to determine how the values of currents change in a single period of sinusoidal quantity, calculations are made by varying the angle of the phase current at steps of 10° ; i.e., $\Delta \omega t = 10^\circ$.

Instantaneous phase current values of a symmetrical current system are interconnected, as follows:

$$\begin{cases} i_A = I_m \sin(\omega t), \\ i_B = I_m \sin(\omega t - 120^\circ), \\ i_C = I_m \sin(\omega t + 120^\circ); \end{cases} \quad (3)$$

where I_m is the maximum amplitude value of the phase current, in A.

The 400 kV double-circuit power transmission line has a maximum effective linear current $I_1 = I_f = 2500$ A; thus, the value of the amplitude phase current I_{mf} is as follows: $I_m = I_1 \cdot \sqrt{2} = 3540$ A.

Using Equation (3), instantaneous current values are calculated at steps of $\Delta\omega t = 10^\circ$.

$$H_{in} = \frac{\pm i_{in}}{2\pi r_{in}}; \quad (4)$$

where i_{in} ($i = A, B, C$) ($n = 1, 2$) shows the phase current flowing through the conductor, which is calculated with Equation (3), r_{in} ($i = A, B, C$) ($n = 1, 2$) are the lengths of distances from phases and their reflections to the reference point M, in m., which are calculated from Figure 2, and H_{in} is the magnetic field strength, in A/m.

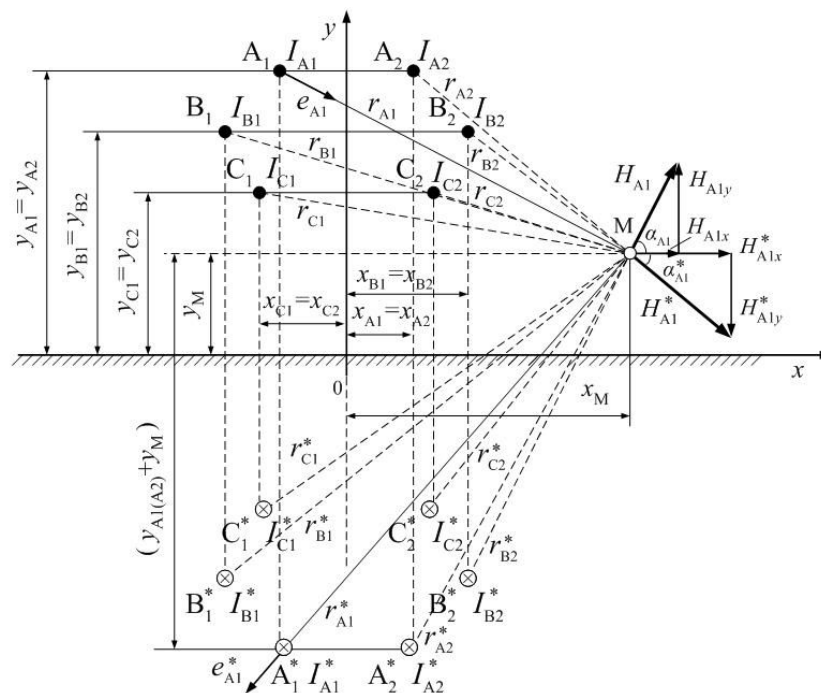


Figure 2. Components of the magnetic field vectors at the point M.

The magnetic field strength generated by the double-circuit three-phase 400 kV overhead transmission line in the plane in Figure 2 is calculated as follows:

$$H_M = \sqrt{H_{Minx}^2 + H_{Miny}^2}; \quad (5)$$

where H_{Minx} and H_{Miny} are the constituents of the magnetic field strength vectors with respect to x and y axes.

Next, we must examine how the values of H vary with the measurement point M moving between the phase conductors of the power line. The location of point M with respect to the ground is $y_0 = y_M$.

The vectors of the magnetic field strength generated at point M are H_{in} and H_{in}^* ($i = A, B, C$) ($n = 1, 2$). After distributing the directions of x and y axes, the following is obtained:

$$H_x = H_{A1x} + H_{B1x} + H_{C1x} + H_{A2x} + H_{B2x} + H_{C2x} + H_{A1x}^* + H_{B1x}^* + H_{C1x}^* + H_{A2x}^* + H_{B2x}^* + H_{C2x}^* \quad (6)$$

$$H_y = H_{A1y} + H_{B1y} + H_{C1y} + H_{A2y} + H_{B2y} + H_{C2y} + H_{A1y}^* + H_{B1y}^* + H_{C1y}^* + H_{A2y}^* + H_{B2y}^* + H_{C2y}^* \quad (7)$$

Assuming that constituents of the magnetic field strength vectors at the observation point M are as follows,

$$E_{Minx} = \sqrt{\frac{1}{T} \sum_{i=1}^n E_{Minx\ max'}^2} \quad (8)$$

$$E_{Miny} = \sqrt{\frac{1}{T} \sum_{i=1}^n E_{Miny\ max'}^2} \quad (9)$$

the effective value of magnetic field strength at observation point M H_M is calculated using Equation (5). One millionth of a Tesla ($1 \mu\text{T}$) corresponds to 0.8 A/m .

As initial phases of conductors in the double-circuit symmetric 400 kV overhead power line are different by 120° , the total magnetic field will be a rotating one, and for the magnetic field vector, at any observation point M, the time course will define an ellipse in a general way. The normal value of the rotating magnetic field strength is assumed to be the effective value of the sinusoid, the amplitude of which is equal to the semi-major axis of the ellipse orbited by the strength vector at the given point.

To express respective constituents of the magnetic field strength (see Figure 2), the following markings are introduced: coordinate y of point M, y_M ; height of the conductors above the ground surface, $y_{A1} = y_{A2}$, $y_{B1} = y_{B2}$, $y_{C1} = y_{C2}$. The phase reflections A_1^* , B_1^* , C_1^* , A_2^* , B_2^* , C_2^* are situated at the same distances above the ground surface in the direction of the y axis. The distances from the conductors to the point M in the direction of the x axis are as follows:

1. $x_{A1M} = x_{A1} + x_M$ is the distance from phase A_1 to point M;
2. $x_{B1M} = x_{B1} + x_M$ is the distance from phase B_1 to point M;
3. $x_{C1M} = x_{C1} + x_M$ is the distance from phase C_1 to point M;
4. $x_{A2M} = x_M - x_{A2}$ is the distance from phase A_2 to point M;
5. $x_{B2M} = x_M - x_{B2}$ is the distance from phase B_2 to point M;
6. $x_{C2M} = x_M - x_{C2}$ is the distance from phase C_2 to point M.

The conductors' phase reflections A_1^* , B_1^* , C_1^* , A_2^* , B_2^* , C_2^* are situated at the same distances in the direction of the x axis.

Figure 2 shows that magnetic field strength vector H_{in} is distributed into two vectors as follows: vector H_{iny} , which varies following the law of sines; and vector H_{inx} , which varies following the law of cosines. The magnetic field strength reflection vector H_{in}^* is distributed analogically. The numerical values of the constituents H_{inx} , H_{inx}^* , H_{iny} , and H_{iny}^* ($i = A, B, C$) ($n = 1, 2$) are found as follows:

$$H_{inx} = H_{in} \cos \alpha_{in} \quad (10)$$

$$H_{inx}^* = H_{in}^* \cos \alpha_{in}^* \quad (11)$$

$$H_{iny} = H_{in} \sin \alpha_{in} \quad (12)$$

$$H_{iny}^* = H_{in}^* \sin \alpha_{in}^* \quad (13)$$

The values of the angles α_{in} and α_{in}^* ($i = A, B, C$) ($n = 1, 2$) are used to consider the positions of the conductor phases and their reflections of the double-circuit 400 kV overhead power line as well as the position of the reference point M with respect to the ground surface and their distances. The values of these trigonometric functions are found from Figure 2. In the general case, these angles α_{in} , α_{in}^* are calculated in the following sequence:

1. The angle α_{in} or α_{in}^* is deduced from the conductor phase under investigation or its reflection's magnetic field vector H_{in} and measurement point M's position with respect to the ground surface.
2. The arctan function of the angle α_{in} or α_{in}^* ($i = A, B, C$) ($n = 1, 2$) is calculated as follows:

$$\alpha_{in} = \arctan \frac{y_{in} - y_M}{x_{inM}}, \tag{14}$$

$$\alpha_{in}^* = \arctan \frac{y_{in} + y_M}{x_{inM}}. \tag{15}$$

3. The functions $\cos\alpha_{in}$ and $\sin\alpha_{in}$ of angles α_{in} or α_{in}^* are calculated with the sign “±” depending on the trigonometric function $\cos\alpha_{in}$ and $\sin\alpha_{in}$ quarter in which the phase load electric field vector H_{in} is calculated.

For the purpose of the mathematical calculation of the magnetic field strength, a 400 kV double-circuit three-phase AC conductor system was selected, which was laid out vertically starting from the ground surface as follows: 1. $C_1(C_2)$ is at a height of 10 m; 2. $C_1(C_2)$ and $B_1(B_2)$ are at a height of 18 m; 3. $B_1(B_2)$ and $A_1(A_2)$ are at a height of 26 m.

The following are the horizontal distances between the different link phases of the conductor: 1. 12 m between A_1 and A_2 ; 2. 16 m between B_1 and B_2 ; 3. 13 m between C_1 and C_2 .

Measurement point M is located 1.5 m vertically from the ground surface. In order for the obtained results of the mathematical calculations to be as precise as possible, 15 total positions of the measurement point M were selected, which were spaced by 5 m and located at 1.5 m vertically from the ground surface (see Figure 3).

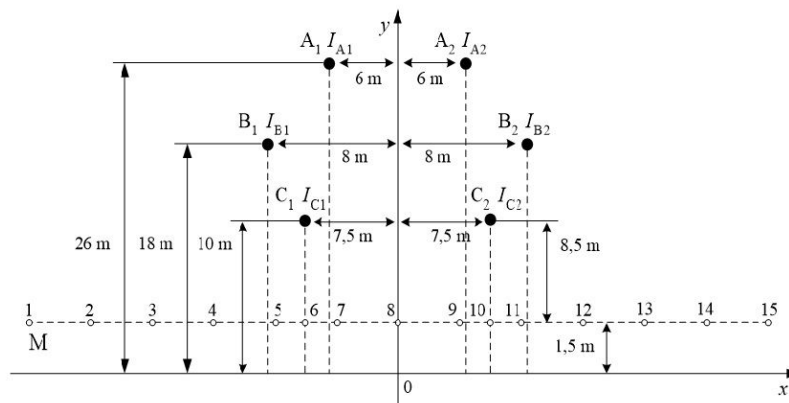


Figure 3. Positions of the measurement point M.

In this paper, extra high-voltage, double-circuit power transmission lines are studied; all six groups with six types of conductor transmission line transpositions are included in the case of long-distance distribution. For 400 kV AC lines, there are six types of first group transposition. There are 36 different transposition layouts possible of the phases in 400 kV double-circuit overhead power lines. For these six different groups of phase conductor transpositions, changes in their transposition sequences influence the results of mathematical calculations [1,24]. The six groups of transposition are as follows (see Figure 1):

- Group 1 ($A_1 - C_2, B_1 - B_2, C_1 - A_2$);
- Group 2 ($B_1 - C_2, A_1 - B_2, C_1 - A_2$);
- Group 3 ($A_1 - C_2, C_1 - B_2, B_1 - A_2$);
- Group 4 ($C_1 - C_2, A_1 - B_2, B_1 - A_2$);
- Group 5 ($B_1 - C_2, C_1 - B_2, A_1 - A_2$);
- Group 6 ($C_1 - C_2, B_1 - B_2, A_1 - A_2$).

5. Discussion

The results obtained from mathematical calculations of the magnetic field in the selected locations of point M_i are presented mathematically in Table 1. The mathematical calculation results in Table 1 suggest that the magnetic field strength achieves its maximum values at points M_6 and M_{11} , and these values are grouped into six categories with six types of conductor transposition.

Table 1. The mathematical calculation of the effective values of the magnetic field strength at 1.5 m above the ground.

Point No.	Distance [m]	Group 1 [A/m]	Group 2 [A/m]	Group 3 [A/m]	Group 4 [A/m]	Group 5 [A/m]	Group 6 [A/m]
M_1	0	2.63	2.85	3.14	2.76	2.76	2.95
M_2	5	4.51	4.66	5.23	4.75	4.94	5.42
M_3	10	8.84	9.12	9.41	8.74	9.79	9.6
M_4	15	18.18	19.67	19.95	19.48	21.38	22.33
M_5	20	35.72	37.05	35.63	40.38	40.85	41.8
M_6	22	39.48	41.33	38.48	46.08	44.65	47.5
M_7	25	32.9	35.15	31.83	43.7	41.33	45.6
M_8	30	18.8	18.53	9.5	35.63	30.88	38.0
M_9	35	37.13	31.35	31.83	43.7	41.33	45.6
M_{10}	38	42.3	38.0	38.48	46.08	44.65	47.5
M_{11}	40	37.6	34.2	35.63	40.38	40.85	41.8
M_{12}	45	19.72	18.81	19.95	19.49	21.38	22.33
M_{13}	50	9.21	8.74	9.41	8.74	9.79	9.6
M_{14}	55	4.8	4.37	5.23	4.75	4.94	5.42
M_{15}	60	3.01	2.47	3.14	2.76	2.76	2.95

These points of observation are situated near phases B_1 and B_2 and between phases C_1 and C_2 of the double-circuit 400 kV overhead power line conductor system. The observation point M_8 is at the very centre of the 400 kV overhead power line (see Figure 3). At this particular point, the magnetic field strength values are lower.

These points of observation are situated near phases B_1 and B_2 and between phases C_1 and C_2 of the double-circuit 400 kV overhead power line conductor system. The observation point M_8 is at the very centre of the 400 kV overhead power line (see Figure 3). At this particular point, the magnetic field strength values are also lower.

The obtained analytical results were also verified through a simulation using the software package COMSOL Multiphysics 3.5. The model simulation additionally assessed the marginal and ambient conditions [6]. Results obtained from a finite element method (FEM) simulation of the magnetic field in the selected locations of point M_i are presented mathematically in Table 2. The FEM simulation results in Table 2 suggest that the magnetic field strength reaches its maximum values at points M_6 and M_{11} , and these values are also grouped into six categories with six types of conductor transposition.

The results of the simulation (see the upper curve of Figure 4) were found to be close to the analytical results; consequently, the proposed methodology can be used to investigate the relevant magnetic field. The assessment of our findings and the obtained results lead us to the following suggestions: the mean error between the analytical findings and simulation results is below 4%. The methodology described here allows the calculation of the magnetic field strength at any point under the three-phase double-circle power transmission line.

The graph in Figure 4 shows that as the measurement point M_i gets farther from the outside phases of the double-circuit 400 kV overhead power line conductor system, the magnetic field strength decreases proportionally. However, at the distance of 12 m from phases B_1 and B_2 , the magnetic field strength still exceeds 16 A/m (i.e., B is more than 20 μ T).

The assessment of the calculation results revealed that values of the magnetic field strength exceed the numerical values established in the EU Hygiene Standard HN 104:2011. The regulation on the

hygienic norms of the European Union and of the Republic of Lithuania states that the numerical values of the electromagnetic field parameters of electric power transmission lines in residential and public buildings—as well as in residential areas—should never exceed the permissible values provided for in EU HN 104:2011.

Table 2. The finite element method (FEM) simulation of the effective values of the magnetic field strength at 1.5 m above the ground.

Point No.	Distance [m]	Group 1 [A/m]	Group 2 [A/m]	Group 3 [A/m]	Group 4 [A/m]	Group 5 [A/m]	Group 6 [A/m]
M ₁	0	2.8	3.0	3.3	2.9	2.9	3.1
M ₂	5	4.8	4.9	5.5	5.0	5.2	5.7
M ₃	10	9.4	9.6	9.9	9.2	10.3	10.1
M ₄	15	20.0	20.7	21.0	20.5	22.5	23.5
M ₅	20	38.0	39.0	37.5	42.5	43.0	44.0
M ₆	22	42.0	43.5	40.5	48.5	47.0	50.0
M ₇	25	35.0	37.0	33.5	46.0	43.5	48.0
M ₈	30	20.0	19.5	10.0	37.5	32.5	40.0
M ₉	35	39.5	33.0	33.5	46.0	43.5	48.0
M ₁₀	38	45.0	40.0	40.5	48.5	47.0	50.0
M ₁₁	40	40.0	36.0	37.5	42.5	43.0	44.0
M ₁₂	45	21.0	19.8	21.0	20.5	22.5	23.5
M ₁₃	50	9.8	9.2	9.9	9.2	10.3	10.1
M ₁₄	55	5.1	4.6	5.5	5.0	5.2	5.7
M ₁₅	60	3.2	2.6	3.3	2.9	2.9	3.1

When locations are identified in which the magnetic field strength values are exceeded, the regulation on the hygienic norms of the European Union and of the Republic of Lithuania obliges operators of the power transmission system, who are responsible for the power transmission lines in operation, to ensure that the permissible values of the electromagnetic field parameters provided for in EU Hygiene Standard HN 104:2011 are adhered to. If the electromagnetic field parameters are found to exceed permissible values, it is compulsory to undertake appropriate actions and to reduce the values of the electromagnetic field parameters to the levels allowed.

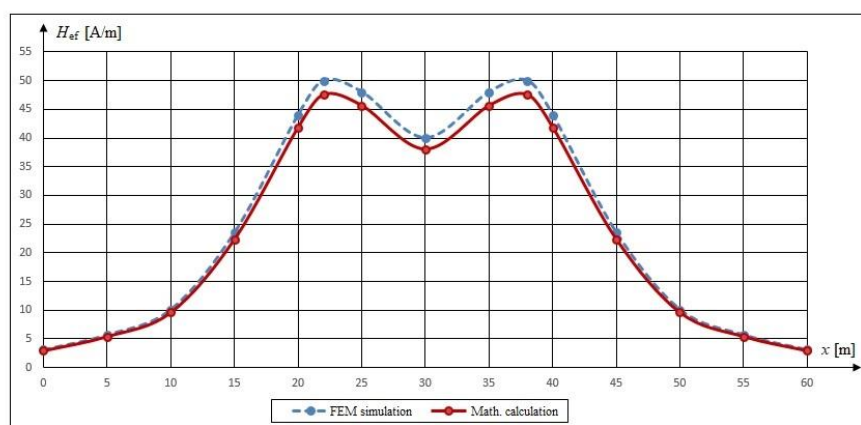


Figure 4. Distribution of the six groups of effective values of magnetic field strength at 1.5 m above the ground, obtained through calculation and FEM simulation.

With the aim of reducing the potential hazards to human health and to ensure safe living conditions in residential areas, it is suggested that experimental measurements of electromagnetic fields should be undertaken in locations or areas with the maximum exposure to electrical or magnetic fields. To mitigate the values of such magnetic fields, it is also recommended that the height of support

bars should be increased or that any individual or commercial activities in their surroundings should be restricted.

6. Conclusions

The magnetic field strength of this power line was found to exceed the numerical values permitted by the Hygiene Standard HN 104:2011 HN, revealing that any person living or working in these areas was in serious danger. Any individual or commercial activities performed by the residents closer than 15 m to the double-circuit 400 kV overhead power line must be restricted.

For these reasons, the magnetic field in these locations must be reduced by installing higher support bars, and persons must wear appropriate personal protective equipment to protect them from exposure to electromagnetic field. For the purpose of more comprehensive analysis, it is recommended that experimental measurements should be made.

The distribution of the magnetic field strength at the high-voltage, double-circuit transmission line could be calculated using the methods of the magnetostatic field or by simulation using the finite element method (FEM). The difference is less than 5% between the results of the mathematical calculation and FEM simulation.

This paper has studied the magnetic field distribution resulting from all six groups with six types of long-distance distributing transposition. As a result, we can see how the impact of the calculation of the six groups' long-distance distribution transposition changes the magnetic field surrounding the transmission line.

The developed mathematical model for the calculation of the magnetic field generated by the conductors in the double-circuit 400 kV overhead power line can be used for the identification of hazardous areas and cases of electromagnetic pollution.

Author Contributions: Conceptualization, R.D.; Methodology, R.L.; Software, R.D.; Validation, R.L.; Formal analysis, R.D.; Investigation, R.D., R.L.; Resources, R.L.; Data curation, R.L.; Writing—Original draft preparation, R.L.; Writing—Review and editing, R.D., R.L.; Visualization, R.L.; Supervision, R.L. All authors have read and agreed to the published version of the manuscript.

Funding: This research received no external funding.

Conflicts of Interest: The authors declare no conflict of interest.

References

1. Safigianni, A.S.; Tsompanidou, C.G. Measurements of electric and magnetic fields due to the operation of in door power distribution substations. *IEEE Trans. Power Deliv.* **2005**, *20*, 1800–1805. [[CrossRef](#)]
2. Jin, J.-M. *Theory and Computation of Electromagnetic Fields*; IEEE Press: Champaign, IL, USA, 2010; pp. 399–410.
3. Haiqi, Y.; Miaoyong, Z. Three-Dimensional Magnetohydrodynamic Calculation for Coupling Multiphase Flow in Round Billet Continuous Casting Mold with Electromagnetic Stirring. *IEEE Trans. Magn.* **2010**, *46*, 82–86. [[CrossRef](#)]
4. Velickovic, D.; Aleksic, S.; Bozic, M. Electromagnetic field in power line surroundings. *Facta Univ. Work. Living Environ. Prot.* **1996**, *1*, 69–79.
5. Dezelak, K.; Jakl, F.; Stumberger, G. Arrangements of overhead power line phase conductors obtained by differential evolution. *Electr. Power Syst. Res.* **2011**, *81*, 2164–2170. [[CrossRef](#)]
6. Deltuva, R.; Lukočius, R. Electric and magnetic field of different transpositions of overhead power line. *Arch. Electr. Eng. J. Pol. Acad. Sci.* **2017**, *66*, 595–605. [[CrossRef](#)]
7. Olsen, R.G.; Deno, D. Magnetic fields from electric power lines: theory and comparison to measurements. *IEEE Trans. Power Deliv.* **1998**, *3*, 2127–2136. [[CrossRef](#)]
8. El Dein, A.Z. Magnetic Field Calculation Under EHV Transmission Lines for More Realistic Cases. *IEEE Trans. Power Deliv.* **2009**, *24*, 2214–2222. [[CrossRef](#)]
9. Begamudre, R.D. *Extra High Voltage AC. Transmission Engineering*, 3rd ed.; Wiley Press: New York, NY, USA, 2006; pp. 172–205.

10. Brandão Faria, J.A.; Almeida, M.E. Accurate Calculation of Magnetic Field Intensity Due to Overhead Power Lines with or without Mitigation Loops with or without Capacitor Compensation. *IEEE Trans. Power Deliv.* **2007**, *22*, 951–959. [[CrossRef](#)]
11. Havas, M. Intensity of electric and magnetic fields from power lines within the business district of 60 Ontario communities. *Sci. Total Environ.* **2002**, *298*, 183–206. [[CrossRef](#)]
12. Peric, M.; Ilic, S.; Aleksic, S. Electromagnetic field analysis in vicinity of power lines. *Elektrotech. Elektron.* **2008**, *1112*, 51–56.
13. Iyyuni, G.B.; Sebo, S.A. Study of transmission line magnetic fields. In Proceedings of the Twenty-Second Annual North American, IEEE Power Symposium, Auburn, AL, USA, 15–16 October 1990; pp. 222–231.
14. Abdel-Salam, M.; Abdallah, H.; El-Mohandes, M.T.; El-Kishky, H. Calculation of magnetic fields from electric power transmission lines. *Electr. Power Syst. Res.* **1999**, *49*, 99–105. [[CrossRef](#)]
15. Ege, Y.; Kalender, O.; Nazlibilek, S. Electromagnetic Stirrer Operating in Double Axis. *IEEE Trans. Ind. Electron.* **2010**, *57*, 2444–2453. [[CrossRef](#)]
16. Nicolaou, Ch.P.; Papadakis, A.P.; Razis, P.A.; Kyriacou, G.A.; Sahalos, J.N. Measurements and predictions of electric and magnetic fields from power lines. *Electr. Power Syst. Res.* **2011**, *81*, 1107–1116. [[CrossRef](#)]
17. Li, L.; Yougang, G. Analysis of magnetic field environment near high voltage transmission lines. In Proceedings of the International Conferences on Communication Technology, Beijing, China, 22–24 October 1998; pp. S26-05-1–S26-05-5.
18. Dahab, A.A.; Amoura, F.K.; Abu-Elhajja, W.S. Comparison of magnetic field distribution of noncompact and compact parallel transmission line configurations. *IEEE Trans. Power Deliv.* **2005**, *20*, 2114–2118. [[CrossRef](#)]
19. Sadiku, M.N.O. *Numerical Techniques in Electromagnetics*; CRC Press: New York, NY, USA, 2001; pp. 743–793.
20. Stewart, J.R.; Dale, S.J.; Klein, K.W. Magnetic field reduction using high phase order lines. *IEEE Trans. Power Deliv.* **1993**, *8*, 628–636. [[CrossRef](#)]
21. Jin, J.-M. *The Finite Element Method in Electromagnetics*, 3rd ed.; Wiley-IEEE Press: New York, NY, USA, 2014; pp. 661–735.
22. Mamishev, A.V.; Nevels, R.D.; Russell, B.D. Effects of conductor sag on spatial distribution of power line magnetic field. *IEEE Trans. Power Deliv.* **1996**, *11*, 1571–1576. [[CrossRef](#)]
23. Chari, M.V.K.; Salon S.J. *Numerical Methods in Electromagnetism*; Academic Press: New York, NY, USA, 2000; pp. 1–61.
24. Hunt, R.W.; Zavalin, A.; Bhatnagar, A.; Chinnasamy, S.; Das, K.C. Electromagnetic biostimulation of living cultures for biotechnology, biofuel and bioenergy applications. *Int. J. Mol. Sci.* **2009**, *10*, 4515–4558. [[CrossRef](#)] [[PubMed](#)]



© 2020 by the authors. Licensee MDPI, Basel, Switzerland. This article is an open access article distributed under the terms and conditions of the Creative Commons Attribution (CC BY) license (<http://creativecommons.org/licenses/by/4.0/>).